

# On primordial universe in anti-de Sitter landscape

Pu-Xin Lin<sup>1,2\*</sup>, Jun Zhang<sup>3†</sup>, and Yun-Song Piao<sup>1,3,4,5‡</sup>

<sup>1</sup> *School of Physics, University of Chinese Academy of Sciences, Beijing 100049, China*

<sup>2</sup> *Department of Physics, University of Wisconsin-Madison,  
1150 University Ave, Madison, WI 53706, U.S.A.*

<sup>3</sup> *International Center for Theoretical Physics Asia-Pacific, Beijing/Hangzhou, China*

<sup>4</sup> *School of Fundamental Physics and Mathematical Sciences,  
Hangzhou Institute for Advanced Study,  
UCAS, Hangzhou 310024, China and*

<sup>5</sup> *Institute of Theoretical Physics, Chinese Academy of Sciences,  
P.O. Box 2735, Beijing 100190, China*

## Abstract

How the spacetime evolved non-perturbatively in a landscape with multiple anti-de Sitter (AdS) vacua, which is theoretically well-motivated, has always been a matter of concern. As a step towards this issue, we perform the (3+1)D numerical relativity simulation for the inhomogeneous universe in an AdS landscape, and find that large inhomogeneity of scalar field can develop into not only sphere-like bubbles, but also novel tube-like structures. It is observed clearly that the bubble or tube wall (across the potential barrier) likely inflates as a quasi-dS space, while the different regions separated by the walls are in different AdS vacua and will collapse towards singularity.

PACS numbers:

---

\* linpiaoxin17@mailsucas.ac.cn

† zhangjun@ucas.ac.cn

‡ yspiao@ucas.ac.cn

## I. INTRODUCTION

The success of inflation [1–5], consistent with current cosmological observations, suggests the existence of a de Sitter (dS) phase in the very early stage of our observable Universe. In string theory, although it is possible that dS vacua exist [6, 7], the construction of such vacua in string landscape is not straightforward. In contrast, anti-de Sitter (AdS) vacua are easy to construct and are ubiquitous. Recently, it has been showed that AdS spacetime not only plays crucial roles as insights into our Universe, e.g.[8–13] but also have potential observable imprints [14–17].

The initial state of the universe might be highly inhomogeneous [18], i.e. the scalar field or spacetime metric can exhibit non-perturbative inhomogeneities before a region of space arrives at a certain vacuum, so that initially well-defined background in such highly inhomogeneous states dose not exist. It is also often speculated that due to the past incompleteness of inflation [19], large fluctuations of spacetime will be inevitably excited near the initial cosmological singularity, in which case the initial conditions are chaotic [5]. In such a non-perturbatively and highly inhomogeneous spacetime, perturbative calculation is not applicable any more.

In the past decades, numerical relativity (NR) has developed significantly and was applied to studies on the merging of black hole binaries [20–22] and non-perturbative cosmologies, e.g.[23–27]. As pointed out, the study of AdS landscape is theoretically well-motivated. Consequently, the dynamics of non-perturbative evolution of the entire spacetime in such landscape has continued to be a matter of concern, e.g.[28]. It is well-known that the region in a single AdS vacuum is unstable and will eventually collapse into a singularity [29], see also e.g.[30]. However, in an AdS landscape, the dynamics and evolution of spacetime is far more complicated, exhibiting rich phenomena that has not been well explored thus far.

As a step towards this issue, we perform the (3+1)D NR simulation of the “universe” in a simplified AdS landscape. Despite the application of NR simulations in cosmologies [23, 24, 31–33], few focused on the AdS landscape. To our knowledge, this work is the first full relativistic simulation showing the non-perturbative evolution of spacetime in the AdS landscape. We find novel phenomena not captured by conventional perturbative analysis, see Fig.1, highlighting the irreplaceable role of NR in comprehending the origin of our Universe.

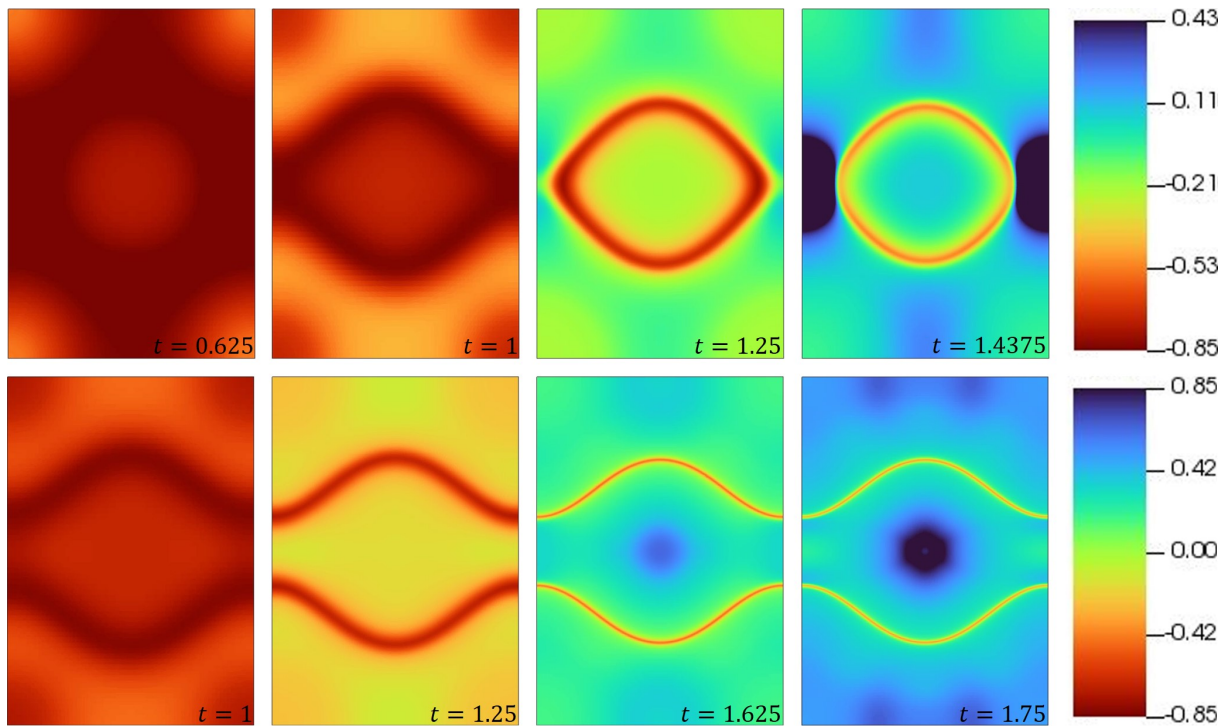


FIG. 1: **Snapshots of spacetime.** The upper and lower panel show how the sphere-like bubbles and tube-like structures form respectively, which are seen in light of the plane passing the center of the grid with normal  $\vec{n} = (1, -1, 0)$ . Initially, the whole space is expanding ( $K < 0$  at the red end of the colorbar). After a period of evolution, different regions of space will be separated by expanding walls (the bubble wall or tube-like “ribbon” at which  $K < 0$ ) into different AdS vacua, while the corresponding AdS regions will collapse ( $K > 0$  with a blue shifted color).

## II. METHOD

Throughout this work, we consider a 1D potential as a phenomenological simplification of the actual complex AdS landscape, setting a fourth-order polynomial barrier between the two AdS minima that have quadratic forms  $\sim \phi^2$  (see Fig.2),

$$V(\phi) = \begin{cases} \frac{1}{2}m_1^2(\phi - \phi_1)^2 + V_1, & \phi < \phi_1, \\ \lambda \left( \phi^2 + \frac{1}{\lambda} \right)^2 - 2\phi^3 - \frac{1}{\lambda} + V_1, & \phi_1 \leq \phi \leq \phi_2, \\ \frac{1}{2}m_2^2(\phi - \phi_2)^2 + V_2, & \phi_2 < \phi, \end{cases} \quad (1)$$

where  $V_1, V_2 < 0$ . Here, we set  $m_1^2 = m_2^2 = 0.2$ ,  $\lambda = 0.49$  ( $c = 8\pi G = 1$ ). We thus have the AdS-like vacua located at  $\phi_1 = 0$  and  $\phi_2 \simeq 2$ , where the potential is constructed to be

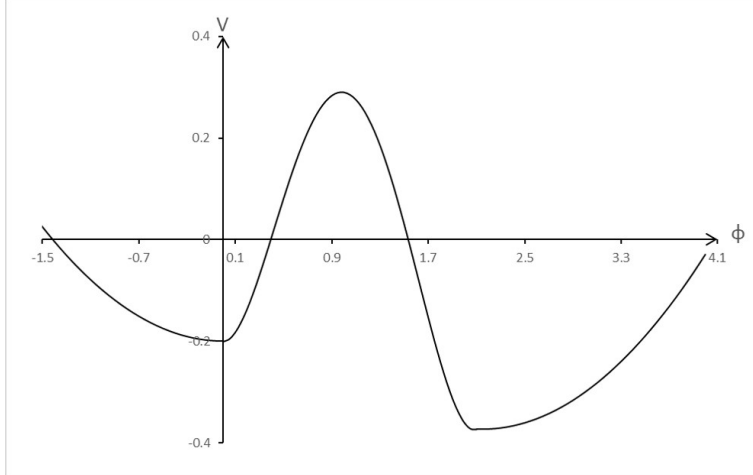


FIG. 2: **A simplified AdS landscape.** The effective potential  $V(\phi)$  has two AdS minima separated by a potential barrier with positive energy.

differentiable, and the maximal value of potential barrier is at  $\phi_b \simeq 1$ .

The large non-perturbative inhomogeneity of fields will be excited inevitably near the initial singularity or the Planck scale, giving rise to the possibility of initially configuration  $\partial_i \phi \partial^i \phi \lesssim 1$ , or  $\Delta\phi \lesssim 1$ . As example, we set the initial inhomogeneity of scalar field as

$$\phi|_{t=0} = \phi_0 + \Delta\phi \sum_{\vec{x}=x,y,z} \cos\left(\frac{2\pi\vec{x}}{L}\right), \quad (2)$$

where the amplitude of inhomogeneity is  $\Delta\phi = \mathcal{O}(0.1)$ , the wavelength of inhomogeneity is taken to be equal to the length of the periodic cubic region (in our simulation  $L = 4$ ).

We modify the NR package GRChombo<sup>1</sup> [34] based on BSSN [35, 36] to perform the simulation. In the context of 3+1 decomposition, the metric is  $g_{00} = -\alpha^2 + \beta_i \beta^i$ ,  $g_{0i} = \beta_i$  and  $g_{ij} = \gamma_{ij}$ , where  $\alpha$  is the lapse parameter,  $\beta^i$  the shift vector and  $\gamma_{ij}$  the spatial metric. The evolutions of  $\tilde{\gamma}_{ij} = \chi \gamma_{ij}$ , the connections  $\tilde{\Gamma}^i = \tilde{\gamma}^{jk} \tilde{\Gamma}_{jk}^i$  and the extrinsic curvature  $K_{ij} = \frac{1}{3} K \delta_{ij} + A_{ij}$  comply with the BSSN equations [35, 36].

Initially <sup>2</sup>, the values of the BSSN variables are set as  $\tilde{\gamma}_{ij} = \delta_{ij}$ ,  $\tilde{A}_{ij} = \chi A_{ij} = 0$ , and  $\chi = 1$ , which is then relaxed in the light of  $\partial_t \chi = \mathcal{H}$  to satisfy the constraints. The scalar

<sup>1</sup> <http://www.grchombo.org>

<https://github.com/GRChombo>

<sup>2</sup> Here, both the momentum and Hamiltonian constraints must be satisfied

field is initially at rest  $\dot{\phi} = 0$ . The local Hubble rate is

$$H_{local} = \lim_{V \rightarrow 0} \left( \frac{1}{V} \int \frac{\rho(\phi)}{3} dV \right)^{1/2} = -\frac{K}{3}. \quad (3)$$

Here, we set the initial spatial expansion uniform  $K_{init} = -1.08$ .

In the simulation, local collapsing regions can develop diverging metric components, after which numerical calculation is rendered unreliable. The solution is to excise, or more crudely, ignore these regions until the numerical errors propagate to the physically relevant computational grids and hinder the stable calculation of these regions.

### III. RESULTS

The simulation results are presented in Fig.1 and Fig.3. The large inhomogeneity will spawn AdS bubbles in a background of a different AdS vacuum. As expected, if a bubble has subcritical initial radius, it will rapidly shrink and collapse into a black hole<sup>3</sup>, and eventually the whole space will evolve into a single AdS state and collapse integrally, see Fig.3-A. However, if the initial radii of the bubbles are supercritical, the regions with different AdS vacua will coexist, separated by not only near-spherical bubble walls (Fig.3-B) but also, interestingly, infinitely extending tube-like walls (Fig.3-C).

These tube-like walls can be understood more clearly in Fig.1. In our simulation, we replace an infinite space with the periodic boundary condition. Thus when considering inhomogeneities on a specific length scale, we actually expect physics happening in larger scales to be similar everywhere. In light of this argument, the “bubble” in the lower panel of Fig.1 actually correspond to the tube that extend along  $\vec{x} (= x, y, z)$  directions through the region where the periodicity of the initial perturbation modes persists. Such tube-like structure looks “as if” the adjacent spherical cells merged partly.

In our simulation, the initial “universe” is set to be expanding homogeneously (all  $H_{local} = const. > 0$ ). However, eventually different regions will tend to evolve into different AdS vacua and be separated by bubble or tube walls. According to Fig.4, we see that though the AdS regions at both sides of the wall are collapsing, the corresponding walls will still expand

---

<sup>3</sup> According to the GRChombo code, the mass of black hole is  $M \approx 5.7$ , which is associated with the apparent horizon and less than but converges to the actual mass of black hole.

and eventually arrive at a quasi-dS static profile, with implications for the inflation stage responsible for our observable Universe might happen at such walls, e.g.[37, 38].

#### IV. CONCLUSIONS

We performed the full relativistic simulation for non-perturbative evolution of spacetime in an AdS landscape. It is found that large inhomogeneity of a scalar field inclines to develop into sphere-like bubbles, and more unexpectedly, into tube-like structures. A region in a single AdS vacuum is destined to collapse, however, we observe that the spacetime evolution is completely different in the AdS landscape, the bubble or tube walls might inflate forever as a quasi-dS space, while the different regions separated by the walls are in different AdS vacua and will collapse towards singularity.

Although the AdS potential serving our simulation is largely simplified, it suffices to capture the essentials of non-perturbative phenomenology of spacetime in the AdS landscape. In a relevant scenario, the inflating region can be surrounded by AdS spacetime, see also [33], thus it is possible to encode the information of inflation in the dual CFT [39], see also [10]. In addition, we can expect that simulations in a more realistic and generic landscape would enable us to acquire a deeper insight into the origin of our observable Universe.

**Acknowledgment** This work is supported by the NSFC No.12075246 and by the Fundamental Research Funds for the Central Universities. We acknowledge the use of GRChombo code for our simulation and the Tianhe-2 supercomputer for providing computing resources. We would like to thank Tiago França, Hao-Hao Li and Hao-Yang Liu for useful discussions.

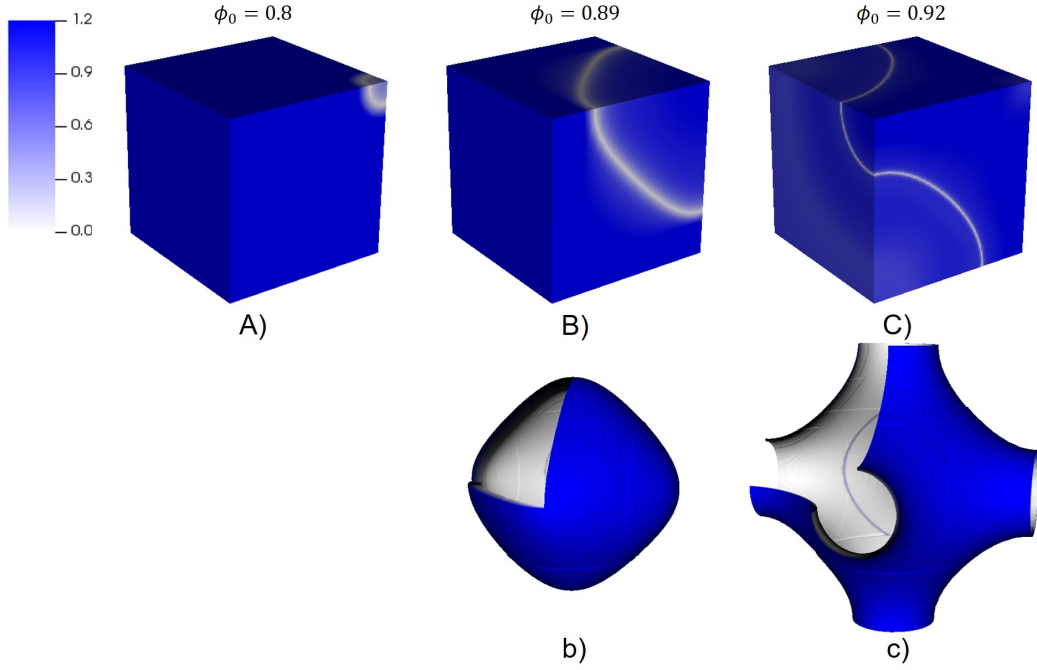


FIG. 3: **The value of  $|\phi - \phi_b|$  (1/8 of the whole computational grid).** In subfig-A, B and C, the lower left and upper right regions correspond to the left and right side of the potential barrier in Fig.2, respectively, and the boundaries colored white mark the position of the barrier. In subfig-A, the snapshot is taken shortly before the upper right AdS region disappears. In subfig-B or C, the snapshot is taken when the bubble or tube wall eventually arrives at rest. The subfig-b and c show the interior of walls with 1/8 of the computational grid removed.

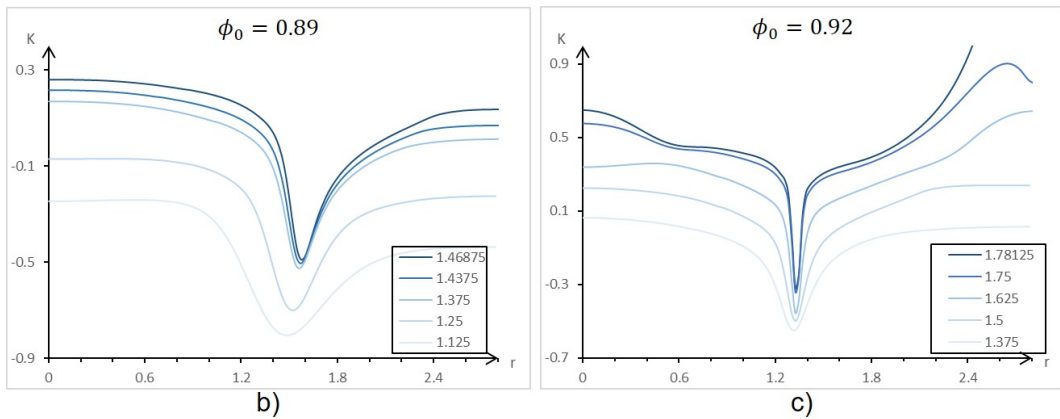


FIG. 4: **The evolution of extrinsic curvature scalar  $K$ .** The horizontal axis is the line from cubic center to the middle point on the edge of whole computational grids (upper right and left vertexes of the boxes in Fig.3). In subfig-b and c, the bubble and tube walls form, and eventually the walls will arrive a quasi-dS stationary profile ( $K = const. < 0$  on wall).

- 
- [1] A. H. Guth, Phys. Rev. D **23**, 347 (1981).
- [2] A. D. Linde, Phys. Lett. B **108**, 389 (1982).
- [3] A. Albrecht and P. J. Steinhardt, Phys. Rev. Lett. **48**, 1220 (1982).
- [4] A. A. Starobinsky, Phys. Lett. B **91**, 99 (1980).
- [5] A. D. Linde, Phys. Lett. B **129**, 177 (1983).
- [6] S. Kachru, R. Kallosh, A. D. Linde, and S. P. Trivedi, Phys. Rev. D **68**, 046005 (2003), hep-th/0301240.
- [7] R. Kallosh, A. Linde, E. McDonough, and M. Scalisi, JHEP **03**, 134 (2019), 1901.02022.
- [8] Y. Chen, V. Gorbenko, and J. Maldacena, JHEP **02**, 009 (2021), 2007.16091.
- [9] T. Hartman, Y. Jiang, and E. Shaghoulian, JHEP **11**, 111 (2020), 2008.01022.
- [10] A. Levine and E. Shaghoulian (2022), 2204.08503.
- [11] S. Cooper, M. Rozali, B. Swingle, M. Van Raamsdonk, C. Waddell, and D. Wakeham, JHEP **07**, 065 (2019), 1810.10601.
- [12] S. Antonini, P. Simidzija, B. Swingle, and M. Van Raamsdonk (2022), 2203.11220.
- [13] S. Antonini, P. Simidzija, B. Swingle, and M. Van Raamsdonk (2022), 2206.14821.
- [14] G. Ye and Y.-S. Piao, Phys. Rev. D **101**, 083507 (2020), 2001.02451.
- [15] G. Ye and Y.-S. Piao, Phys. Rev. D **102**, 083523 (2020), 2008.10832.
- [16] J.-Q. Jiang and Y.-S. Piao, Phys. Rev. D **104**, 103524 (2021), 2107.07128.
- [17] G. Ye, J. Zhang, and Y.-S. Piao (2021), 2107.13391.
- [18] J. Feldbrugge, J.-L. Lehners, and N. Turok, Phys. Rev. Lett. **119**, 171301 (2017), 1705.00192.
- [19] A. Borde, A. H. Guth, and A. Vilenkin, Phys. Rev. Lett. **90**, 151301 (2003), gr-qc/0110012.
- [20] F. Pretorius, Phys. Rev. Lett. **95**, 121101 (2005), gr-qc/0507014.
- [21] M. Campanelli, C. O. Lousto, P. Marronetti, and Y. Zlochower, Phys. Rev. Lett. **96**, 111101 (2006), gr-qc/0511048.
- [22] J. G. Baker, J. Centrella, D.-I. Choi, M. Koppitz, and J. van Meter, Phys. Rev. Lett. **96**, 111102 (2006), gr-qc/0511103.
- [23] J. T. Giblin, J. B. Mertens, and G. D. Starkman, Phys. Rev. Lett. **116**, 251301 (2016), 1511.01105.
- [24] E. Bentivegna and M. Bruni, Phys. Rev. Lett. **116**, 251302 (2016), 1511.05124.



- [25] N. Musoke, S. Hotchkiss, and R. Easther, *Phys. Rev. Lett.* **124**, 061301 (2020), 1909.11678.
- [26] H. J. Macpherson, P. D. Lasky, and D. J. Price, *Phys. Rev. D* **95**, 064028 (2017), 1611.05447.
- [27] H. J. Macpherson, D. J. Price, and P. D. Lasky, *Phys. Rev. D* **99**, 063522 (2019), 1807.01711.
- [28] J. J. Blanco-Pillado, H. Deng, and A. Vilenkin, *JCAP* **05**, 014 (2020), 1909.00068.
- [29] L. F. Abbott and S. R. Coleman, *Nucl. Phys. B* **259**, 170 (1985).
- [30] P. Bizon and A. Rostworowski, *Phys. Rev. Lett.* **107**, 031102 (2011), 1104.3702.
- [31] W. E. East, M. Kleban, A. Linde, and L. Senatore, *JCAP* **09**, 010 (2016), 1511.05143.
- [32] K. Clough, E. A. Lim, B. S. DiNunno, W. Fischler, R. Flauger, and S. Paban, *JCAP* **09**, 025 (2017), 1608.04408.
- [33] P.-X. Lin and Y.-S. Piao, *Phys. Rev. D* **105**, 063534 (2022), 2111.09174.
- [34] K. Clough, P. Figueras, H. Finkel, M. Kunesch, E. A. Lim, and S. Tunyasuvunakool, *Class. Quant. Grav.* **32**, 245011 (2015), 1503.03436.
- [35] T. W. Baumgarte and S. L. Shapiro, *Phys. Rev. D* **59**, 024007 (1998), gr-qc/9810065.
- [36] M. Shibata and T. Nakamura, *Phys. Rev. D* **52**, 5428 (1995).
- [37] A. Vilenkin, *Phys. Rev. Lett.* **72**, 3137 (1994), hep-th/9402085.
- [38] A. D. Linde, *Phys. Lett. B* **327**, 208 (1994), astro-ph/9402031.
- [39] B. Freivogel, V. E. Hubeny, A. Maloney, R. C. Myers, M. Rangamani, and S. Shenker, *JHEP* **03**, 007 (2006), hep-th/0510046.